

M. NABIALEK*, P. PIETRUSIEWICZ*, M. SZOTA**, A. DOBRZAŃSKA-DANIKIEWICZ***, S. LESZ***,
M. DOŚPIAŁ*, K. BŁOCH*, K. OŹGA****

THE STRUCTURAL STABILITY OF THE $\text{Fe}_{36}\text{Co}_{36}\text{Si}_{19}\text{B}_5\text{Nb}_4$ BULK AMORPHOUS ALLOY

STABILNOŚĆ STRUKTURY MASYWNEGO STOPU AMORFICZNEGO $\text{Fe}_{36}\text{Co}_{36}\text{Si}_{19}\text{B}_5\text{Nb}_4$

In this paper, the results of the investigation into the fractured surface microstructure of the amorphous samples of $\text{Fe}_{36}\text{Co}_{36}\text{B}_{19}\text{Si}_5\text{Nb}_4$ in the shape of rods of diameters: 1 mm, 2 mm and 3 mm in the as-cast state are presented. The samples were prepared by injection of molten alloy into cooled copper dies. The process of diffusion in the investigated material has a different speed depending on the temperature gradient within the volume of the rod. The atomic diffusion leads to the creation of different zones within the rod fracture: the zone in contact with the copper die, the intermediate fracture zone, and the zone in the vicinity of the rod core; the three zones have been found to exhibit different amorphous structures.

Keywords: bulk amorphous alloys, surface, diffusion process, microstructure, fracture surface morphology

W pracy przedstawiono wyniki badań mikrostruktury na powierzchni przełomów próbek $\text{Fe}_{36}\text{Co}_{36}\text{Si}_{19}\text{B}_5\text{Nb}_4$ amorficznych w postaci prętów o średnicy 1 mm, 2 mm i 3 mm, w stanie po zestaleniu. Pręty wytworzono metodą wtlaczania ciekłego stopu do miedzianej, chłodzonej cieżką formy. Proces dyfuzji atomów w badanym materiale charakteryzuje się inną dynamiką w zależności od gradientu temperatury w objętości pręta. Wyróżnia się trzy wyraźnie widoczne strefy: od kontaktu z miedzianą formą, strefę przejściową oraz strefę opisującą rdzeń pręta. Każdą z wyróżnionych stref charakteryzują różne konfiguracje atomów w zakresie stanu amorficznego. Na podstawie badań stwierdzono, że w masywnych materiałach amorficznych występuje fluktuacja składu oraz gęstości w zależności od szybkości chłodzenia.

1. Introduction

The structure of metallic materials is one of their most important properties, [1-3]. It is well-known that many of the properties of metallic alloys depend on their structure, [4-6]. Currently, intensive investigations are being undertaken into a new group of metallic materials: the so-called bulk amorphous materials, [2, 3, 7, 8]. Within these alloys there is no long-distance interaction between atoms and their microstructure is similar to that of a liquid, [9-10]. Therefore, the structural investigation of the bulk amorphous alloys with different thicknesses facilitates, at least in part, the discovery of the mechanism of the change of their microstructure.

2. Materials and Methods

The samples of the investigated alloy, $\text{Fe}_{36}\text{Co}_{36}\text{B}_{19}\text{Si}_5\text{Nb}_4$, were obtained using components with the following purities: Fe – 99.99%, Co – 99.9%, Nb – 99.999%, Si – 99.99% and B – 99.99%. The crystalline ingots of alloy were re-melted several times, in order to ensure thorough mixing of the chemical

constituents. Bulk amorphous samples were prepared using a technique involving injection of molten material into a water-cooled copper die. The samples obtained using the aforementioned technique are each in the form of a rod with a length of 20 mm and diameters of: 1 mm, 2 mm or 3 mm.

The microstructure of the samples in the as-cast state was investigated by means of a Seifert-FPM XRD7 X-ray diffractometer. The diffraction of the Roentgen rays was performed using a copper lamp with $K_{\alpha} = 1.54056 \text{ \AA}$. The samples were scanned in 2θ angle from 30° to 80° , in 0.02° increments and with exposure time of 3 s per step.

Morphology of the rod fractures was investigated by means of a Zeiss Supra25 scanning electron microscope (SEM) under a voltage of 20 kV, with 3,000 times magnification. The chemical composition of the micro-domains in the different rod zones was found by means of a point method using an EDAX energy-dispersive X-ray spectroscope (EDS), coupled with the SEM. The Boron content in the alloy composition was not determined. In order to accomplish this, it would be necessary to present detailed investigation assumptions, a description of the investigated material and the adopted investigation techniques.

* INSTITUTE OF PHYSICS, CZESTOCHOWA UNIVERSITY OF TECHNOLOGY, 19 ARMII KRAJOWEJ AVE., 42-200 CZESTOCHOWA, POLAND

** INSTITUTE OF MATERIAL SCIENCE ENGINEERING, CZESTOCHOWA UNIVERSITY OF TECHNOLOGY, 19 ARMII KRAJOWEJ AVE., 42-200 CZESTOCHOWA, POLAND

*** INSTITUTE OF ENGINEERING MATERIALS AND BIOMATERIALS, SILESIAN UNIVERSITY OF TECHNOLOGY, 18A KONARSKIEGO STREET, 44-100 GLIWICE, POLAND

**** INSTITUTE OF ELECTRONICS AND AUTOMATION SYSTEMS, CZESTOCHOWA UNIVERSITY OF TECHNOLOGY, 17 ARMII KRAJOWEJ AVE., 42-200 CZESTOCHOWA, POLAND

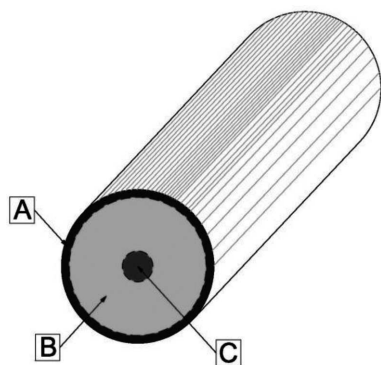


Fig. 1. Sectional view of a rod sample with investigation zones marked from surface to core: A – zones in contact with the copper die; B – intermediate fracture zones; and C – zones in the vicinity of the rod core

All of the X-ray investigations were performed at room temperature on energetically-low powdered samples, facilitating the gaining of information from the whole volume of the material.

3. Results and Discussion

Fig. 2 shows the X-ray diffraction patterns obtained for the samples of the $\text{Fe}_{36}\text{Co}_{36}\text{B}_{19}\text{Si}_5\text{Nb}_4$ alloy in the as-cast state; rod samples of diameters 1 mm, 2 mm, and 3 mm.

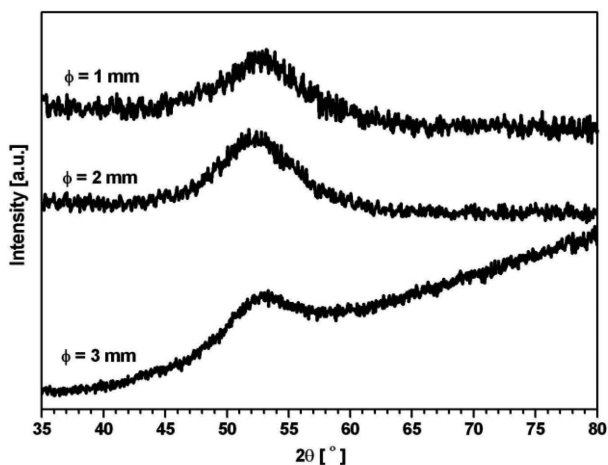


Fig. 2. Diffraction patterns measured for samples of the investigated alloy $\text{Fe}_{36}\text{Co}_{36}\text{B}_{19}\text{Si}_5\text{Nb}_4$ in the as-cast state in the shape of rods of diameters: 1 mm, 2 mm, and 3 mm

All of the diffraction patterns obtained for powdered rods of the investigated alloys are similar and consist only of wide, diffuse maxima; this confirms a lack of crystallites in the sample volume. In crystalline materials, periodic atomic distribution can be observed, where interatomic angular correlations are conserved. This means that in the case of crystalline materials, it is possible to determine accurately the distance between the lattice planes and this is associated with distinctive narrow peaks in the diffraction patterns. The lack of these clear narrow maxima in the X-ray diffraction patterns indicates an aperiodic, chaotic, atomic distribution in the material volume, hence an amorphous structure.

The fracture of the cast rods of the $\text{Fe}_{36}\text{Co}_{36}\text{B}_{19}\text{Si}_5\text{Nb}_4$ alloy, obtained by a bending process, exhibits a different structure, depending on the location of analysis (Figs. 3-5). The fractographic investigations show the characteristic fractures gained for the relaxed amorphous structure of the rods, with diameters 1 mm and 2 mm, of the $\text{Fe}_{36}\text{Co}_{36}\text{B}_{19}\text{Si}_5\text{Nb}_4$ alloy (Fig. 3 a, b, and c for the rod $\Phi = 1$ mm, Fig. 4 a, b, and c for the rod $\Phi = 2$ mm). For the rods $\Phi = 1$ mm and 2 mm, the fractures are smooth, with barely-visible 'striated' and 'vein-like' features both in the zone between the core and surface of the rod (Fig. 3b and 4b) and in the surface zone having contact with the copper die (Fig. 3a and 4a). The results of the fracture observation of the rod with 3 mm diameter of the $\text{Fe}_{36}\text{Co}_{36}\text{B}_{19}\text{Si}_5\text{Nb}_4$ alloy (Fig. 5a, b, and c) showed a similar type of fracture. In the intermediate zone between the core and surface, the fracture is characterised by the presence of small 'scales or flakes' (Fig. 5b) which are typical of fractures of strongly-relaxed metallic glasses.

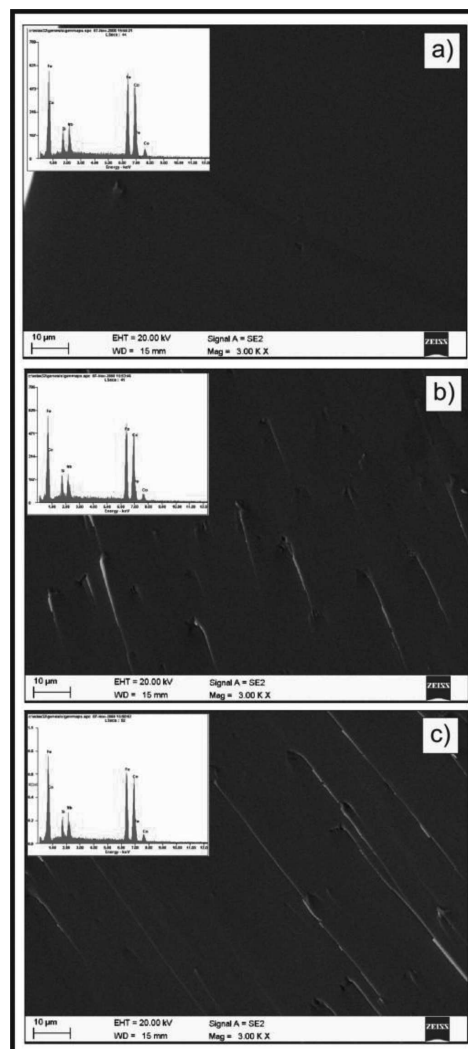


Fig. 3. Morphology of the 1 mm rod fracture of the $\text{Fe}_{36}\text{Co}_{36}\text{B}_{19}\text{Si}_5\text{Nb}_4$ alloy (magnified x3000), with the associated chemical composition analysis within: (a) the outer layer of the rod fracture (smooth fracture with singular localised discontinuities); (b) the intermediate rod fracture zone between outer layer and core (smooth fracture with 'striations'); (c) the rod fracture core (smooth fracture with 'striations')

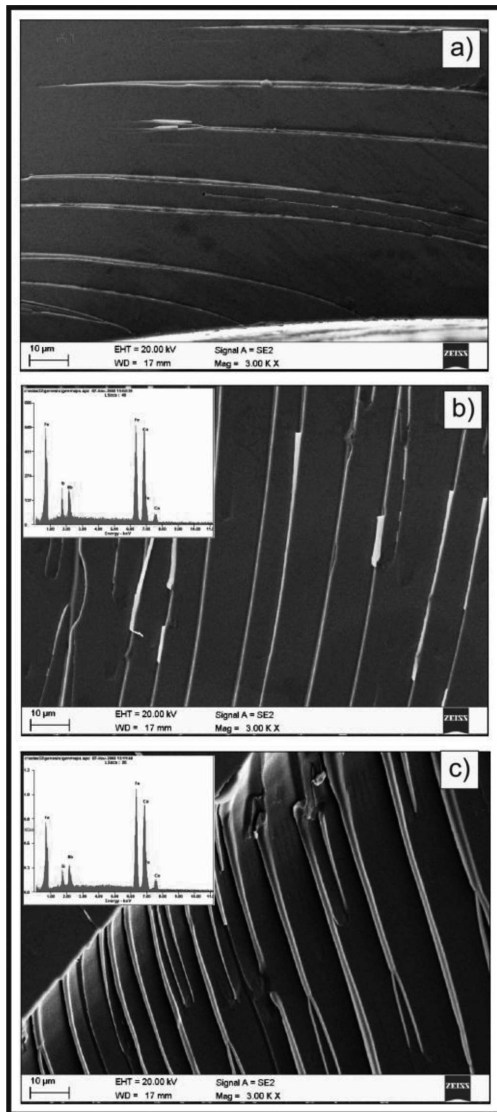


Fig. 4. Morphology of the 2 mm rod fracture of the $\text{Fe}_{36}\text{Co}_{36}\text{B}_{19}\text{Si}_5\text{Nb}_4$ alloy (magnified $\times 3000$), with the associated chemical composition analysis within: (a) the outer layer of the rod fracture (smooth fracture with pronounced striations); (b) the intermediate rod fracture zone between outer layer and core (smooth fracture with clear dense striations); (c) the rod fracture core (mixed fracture: clear division between smooth and highly striated surfaces)

In Figs. 3, 4 and 5, the analysis of the investigated alloy components are shown. This was obtained by a point method using an EDAX EDS, coupled with the SEM. The data obtained from the analysis are shown in Table 1.

TABLE 1

The chemical constituents of the investigated alloy, obtained by point method

Element	Concentration of elements, %at.					
	1 mm		2 mm		3 mm	
Fe	43.87	44.00	43.81	43.44	45.77	44.28
Co	43.69	42.74	42.93	44.38	45.15	43.04
Si	6.81	7.53	7.58	6.91	4.83	6.85
Nb	5.64	5.73	5.68	5.27	4.25	5.82

On the basis of the data shown in Table 1, it can be stated that obtained samples of the $\text{Fe}_{36}\text{Co}_{36}\text{B}_{19}\text{Si}_5\text{Nb}_4$ alloy in the rod form were homogeneous and during their production there was no substantial loss of components.

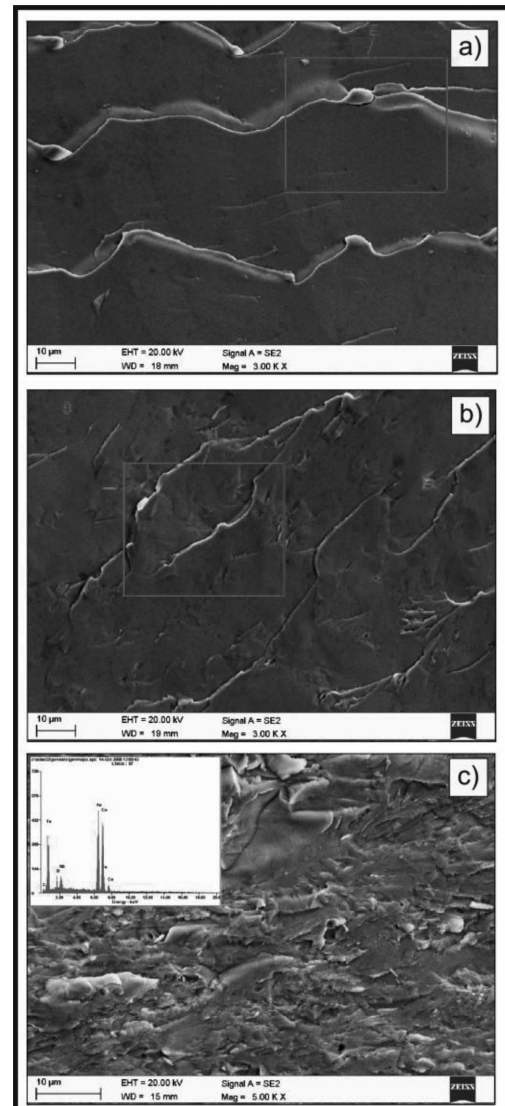


Fig. 5. Morphology of the 3 mm rod fracture of the $\text{Fe}_{36}\text{Co}_{36}\text{B}_{19}\text{Si}_5\text{Nb}_4$ alloy (magnified $\times 3000$), with the associated chemical composition analysis within: (a) the outer layer of the rod fracture (smooth fracture with pronounced undulating striations); (b) the intermediate rod fracture zone between outer layer and core (fracture with dense, scaly, vein-like appearance); (c) the rod fracture core (mixed fracture: weakly developed surface – mostly scaly with light vein-like appearance)

4. Conclusions

The manufactured rods of the $\text{Fe}_{36}\text{Co}_{36}\text{B}_{19}\text{Si}_5\text{Nb}_4$ alloy (with diameters 1, 2 and 3 mm) were fully-amorphous, which was confirmed by the obtained X-ray diffraction patterns and SEM images of the structure of the fracture. The crystallisation process in bulk amorphous alloys of the FeCoSiNbB-type results from the changes in the amorphous matrix, and is related with long-distance atomic diffusion. The images of the rod fracture structure show clearly the gradual, slow changes

progressing in the investigated alloy during solidification. For the rod of 1 mm diameter, the fracture is smooth with only a few, barely visible 'striations'. For the rod of 2 mm diameter, the observed fracture appeared as a band of 'striations' mixed with a smooth fracture. For the rod of 3 mm diameter, locations with 'scales' and 'veins' are visible.

The next stage of metastable changes of the thermodynamically unstable amorphous alloys is certain to be the appearance of crystallisation products with completely different chemical composition compared with the remaining amorphous matrix. On the basis of the analysis of the rod structure images, with 3 mm diameter, it is believed that this rod diameter is the limit for material with a fully amorphous structure.

REFERENCES

- [1] R. Brandel, A. Mokhun, I. Mokhun, J. Viktorovskaja, Fine structure of heterogeneous vector field and its space averaged polarization characteristics, *Optica Applicata* **36**(1), 79-96 (2006).
- [2] M. Hasiak, K. Sobczyk, J. Zbroszczyk, W. Ciurzyńska, J. Olszewski, M. Nabiałek, J. Kaleta, J. Świerczek, A. Łukiewska, Some magnetic properties of bulk amorphous $(\text{Fe}_{61}\text{Co}_{10}\text{Zr}_{2.5}\text{Hf}_{2.5}\text{Ti}_2\text{W}_2\text{B}_{20})_{100-x}\text{Y}_x$ ($x = 0$ or 2) alloy, *IEEE Transactions on Magnetics* **11**, 3879-3882 (2008).
- [3] K. Sobczyk, J. Świerczek, J. Gondro, J. Zbroszczyk, W. Ciurzyńska, J. Olszewski, P. Brągiel, A. Łukiewska, J. Rzącki, M. Nabiałek, Microstructure and Some Magnetic Properties of Bulk Amorphous $(\text{Fe}_{0.61}\text{Co}_{0.10}\text{Zr}_{0.025}\text{Hf}_{0.025}\text{Ti}_{0.02}\text{W}_{0.02}\text{B}_{0.20})_{100-x}\text{Y}_x$ ($x = 0, 2, 3$ or 4), *Journal of Magnetism and Magnetic Materials* **324**, 540-549 (2012).
- [4] D. Malacara, M. Servin, Z. Malacara, *Interferogram Analysis for Optical Testing*, Dekker, 1998.
- [5] K. Kosiel, J. Muszalski, A. Szerling, M. Bugajski, R. Jakieła, Improvement of quantum efficiency of MBE grown AlGaAs/InGaAs/GaAs edge emitting lasers by optimisation of construction and technology, *Vacuum* (in press).
- [6] B. Cichy, P. Psuja, A. Górecka-Drzazga, W. Stręk, J.A. Dziuban, Technology and parameters of cold cathodes made from carbon nanotubes, *Proceedings of IX Conference COE2006*, June 19-22, 2006, Kraków-Zakopane, Poland, pp. 81-84 (in Polish).
- [7] D. Szewieczek, J. Tyrlik-Held, S. Lesz, Changes of mechanical properties and fracture morphology of amorphous tapes involved by heat treatment, *Journal of Materials Processing Technology* **109**, 190-195 (2001).
- [8] S. Lesz, Preparation of Fe-Co-based bulk amorphous alloy from high purity and industrial raw materials, *Archives of Materials Science and Engineering* **48**, 2, 77-88 (2011).
- [9] A. Pusz, A. Januszka, S. Lesz, R. Nowosielski, Thermal conductivity measuring station for metallic glasses, *Archives of Materials Science and Engineering* **47**, 2, 95-102 (2011).
- [10] R. Nowosielski, A. Zajdel, S. Lesz, B. Kostrubiec, Z. Stokłosa, Crystallization of amorphous $\text{Co}_{77}\text{Si}_{11.5}\text{B}_{11.5}$ alloy, *Archives of Materials Science and Engineering* **28**, 3, 141-148 (2007).